

See discussions, stats, and author profiles for this publication at: <https://www.researchgate.net/publication/309367650>

Replication Errors Made During Oogenesis Lead to Detectable De Novo mtDNA Mutations in Zebrafish Oocytes with a Low...

Article in *Genetics* · October 2016

DOI: 10.1534/genetics.116.194035

CITATIONS

0

READS

17

12 authors, including:



[Mike Gerards](#)

Maastricht University

45 PUBLICATIONS 473 CITATIONS

[SEE PROFILE](#)



[Sabina Vanherle](#)

Maastricht University

6 PUBLICATIONS 227 CITATIONS

[SEE PROFILE](#)



[Jo Vanoevelen](#)

Maastricht Universitair Medisch Centrum

38 PUBLICATIONS 1,132 CITATIONS

[SEE PROFILE](#)



[Marc Muller](#)

University of Liège

173 PUBLICATIONS 2,804 CITATIONS

[SEE PROFILE](#)

Some of the authors of this publication are also working on these related projects:



The role of mitochondrial processes in learning and cognition [View project](#)

1 **Replication errors made during oogenesis lead to detectable *de novo* mtDNA**
2 **mutations in zebrafish oocytes with a low mtDNA copy number**

3

4 Auke B.C. Otten*, Alphons P.M. Stassen*, Michiel Adriaens[†], Mike Gerards[†], Richard
5 G.J. Dohmen*, Adriana J. Timmer*, Sabina J.V. Vanherle*, Rick Kamps*, Iris B.W.
6 Boesten*, Jo M. Vanoevelen*, Marc Muller[‡], Hubert J.M. Smeets^{*,†}

7

8

9 *Department of Genetics & Cell Biology, Unit Clinical Genomics, School for Oncology
10 and Developmental Biology (GROW), Maastricht University, 6200MD, Maastricht, the
11 Netherlands

12

13 [†]Maastricht Centre for Systems Biology (MaCSBio), Maastricht University, 6200MD,
14 the Netherlands

15

16 [‡]Laboratory of Organogenesis and Regeneration, GIGA-Resarch, Université de Liège,
17 4000 Liège, Belgium

18

19

20

21

22

23

24

25

26 **Running title: Prevalence of mitochondrial DNA mutations in zebrafish oocytes**

27

28 **Keywords:** Mitochondrial DNA, de novo mutations, Next generation sequencing,

29 zebrafish, oogenesis

30

31 **Corresponding Author:**

32 Hubert J.M. Smeets (HS)

33 Postbus 616 (box 16)

34 6200 MD Maastricht

35

36

37

38

39

40

41

42

43

44

45

46

47

48

49

50 **Abstract**

51 Of all pathogenic mitochondrial DNA (mtDNA) mutations in humans, ~25% is *de*
52 *novo*, although the occurrence in oocytes has never been directly assessed. We
53 used next generation sequencing to detect point mutations directly in the mtDNA of
54 3-15 individual mature oocytes and three somatic tissues from eight zebrafish
55 females. Various statistical and biological filters allowed reliable detection of *de novo*
56 variants with heteroplasmy $\geq 1.5\%$. In total, we detected 38 *de novo* base
57 substitutions, but no insertions or deletions. These 38 *de novo* mutations were
58 present in 19 of 103 mature oocytes, indicating that ~20% of the mature oocytes
59 carry at least one *de novo* mutation with heteroplasmy $\geq 1.5\%$. This frequency of *de*
60 *novo* mutations is close to that deduced from the reported error rate of polymerase
61 gamma, the mitochondrial replication enzyme, implying that mtDNA replication errors
62 made during oogenesis are a likely explanation. Substantial variation in the mutation
63 prevalence among mature oocytes can be explained by the highly variable mtDNA
64 copy number, since we previously reported that ~20% of the primordial germ cells
65 have a mtDNA copy number of ≤ 73 and would lead to detectable mutation loads. In
66 conclusion, replication errors made during oogenesis are an important source of *de*
67 *novo* mtDNA base substitutions and their location and heteroplasmy level determine
68 their significance.

69 **Article Summary**

70 Approximately 25% of the mitochondrial DNA (mtDNA) mutations are thought to
71 occur *de novo*. To detect *de novo* mutations, we screened the mitochondrial DNA of
72 103 zebrafish oocytes. We detected 38 *de novo* base substitutions in ~20% of the
73 zebrafish oocytes tested. The mutation frequency is similar to the reported error rate

74 of the mitochondrial replication enzyme polymerase gamma, suggesting replication
75 errors made during oogenesis are an important source of *de novo* mtDNA mutations.
76 Variation in the mtDNA copy number among oocytes explains the high variation in
77 the prevalence of *de novo* mutations.

78 **Introduction**

79 Comparative sequence analysis of the mitochondrial DNA (mtDNA) has revealed a
80 high degree of variability, much higher than its nuclear counterpart (LYNCH *et al.*
81 2006). This is generally explained by limited recombination and recombination-
82 mediated mtDNA repair events to counteract errors made during mtDNA replication
83 (BARR *et al.* 2005) and the close proximity of the unprotected mtDNA to the oxidative
84 phosphorylation (OXPHOS) machinery, which produces (potentially) mutagenic
85 reactive oxygen species (ROS) (BRAND 2010). As a result, mtDNA mutations are an
86 important cause of a group of devastating inherited diseases (TAYLOR and TURNBULL
87 2005). To date, over 150 pathogenic mtDNA mutations have been identified, as well
88 as many more polymorphisms of unknown significance (HELLEBREKERS *et al.* 2012).
89 As human and animal cells have a high mtDNA copy number, wild-type and variant
90 mtDNA genotypes can co-exist, a state referred to as heteroplasmy. The high mtDNA
91 copy number compensates low-level pathogenic mtDNA mutations and avoids
92 disease manifestation. A pathogenic mtDNA mutation will only manifest if its
93 heteroplasmy value exceeds a certain threshold (HELLEBREKERS *et al.* 2012). The
94 mtDNA inherits maternally, and a female carrying an mtDNA mutation can transmit
95 this mutation to her offspring through the mtDNA of her oocytes.

96 Maternal inheritance of pre-existing mtDNA mutation does not explain all
97 patients suffering from mtDNA mutations. In 25% of these patients, the disease-

98 causing mutation cannot be detected in the maternal mtDNA (SALLEVELT *et al.* 2016).
99 Although we cannot exclude some of these mutation were present at undetectable
100 low-level heteroplasmy levels in the maternal mtDNA, this suggests that most of
101 these mutations have occurred *de novo* during germ line development. The
102 inheritance of the mtDNA occurs through a segregational bottleneck: only a limited
103 number of the mtDNA molecules, the so-called bottleneck size, from the oocyte are
104 transmitted to the (primordial) germline cells (PGCs) of the next generation (CREE *et*
105 *al.* 2008). We hypothesize that, in case of a constant mutation rate, a low mtDNA
106 copy number at the bottom of the bottleneck could lead to *de novo* mutations
107 reaching detectable heteroplasmy levels, which, dependent on the nature of the
108 mutations, can be of functional and/or pathogenic significance. Experimental
109 evidence for this hypothesis has long been difficult to obtain, because of the low
110 heteroplasmy level at which these mutations occur, which were generally below the
111 detection level of conventional sequencing techniques. Over the past decade, next-
112 generation sequencing (NGS) technologies have been developed, allowing an in
113 depth determination of the mutations and heteroplasmy levels directly in the mtDNA
114 of individual oocytes.

115 An estimation of the prevalence of *de novo* mtDNA mutation requires a
116 significant number of oocytes to be sequenced. For both biological and ethical
117 reasons this is difficult to achieve in humans and most animals. In contrast, oocyte
118 collection from zebrafish is relatively easy and efficient and therefore we used
119 zebrafish mature oocytes to assess the *de novo* mtDNA mutation risk. We
120 characterized *de novo* mutations, their location and their heteroplasmy level in 103
121 oocytes and three somatic (maternal) tissues from eight different female zebrafish
122 using NGS with a minimal coverage of 1,700. Furthermore, for all oocytes with one or

123 more *de novo* mutation(s), we estimated the mtDNA copy number at which these
124 mutations arose, based on their heteroplasmy levels. Given the high mtDNA
125 sequence similarity between humans and zebrafish (BROUGHTON *et al.* 2001) and the
126 conservation of the mtDNA bottleneck within the animal kingdom (HOWELL *et al.* 1992;
127 CREE *et al.* 2008; WOLFF *et al.* 2011; LEE *et al.* 2012), our findings have insinuations
128 for the occurrence of *de novo* mtDNA disease in humans.

129 **Materials and Methods**

130 **Zebrafish maintenance and sample collection**

131 Wild-type female zebrafish from the *AB* strain were used. Raising and housing was
132 according to standard procedures at 28°C (KIMMEL *et al.* 1995) in the zebrafish facility
133 of Liège University, where local ethical approval by the committee of Animal
134 Research was obtained. Mature unfertilized oocytes were collected by squeezing the
135 abdomen of anaesthetized females. The oocytes used were normal in morphological
136 appearance. After oocyte collection, the female fish were sacrificed in ice-cold water,
137 after which biopsies of brain, liver and muscle were obtained. An overview of the 127
138 samples is given in Table 1.

139 **Table 1. Overview of samples collected**

Zebrafish #	1	2	3	4	5	6	7	8
Biopsies	3	3	3	3	3	3	3	3
Number of oocytes	3	13	15	14	15	14	15	14

140 **Isolation procedure of mtDNA**

141 Oocytes were collected in sterile tubes and lysed for 4 hours at 50°C in 500 µl DNA
142 lysis buffer containing 75 mM NaCl, 50 mM EDTA, 20 mM HEPES, 0.4% SDS and

143 200 µg proteinase K (Sigma). Subsequently, isopropanol was added and samples
144 were precipitated overnight at -20°C. After thorough centrifugation, the DNA pellet
145 was washed with 70% ethanol and dissolved in TE buffer. The biopsies of brain, liver
146 and muscle from the adult female fish were collected in sterile tubes containing
147 Nuclei Lysis solution from the Wizard Genomic Purification Kit (Promega).
148 Subsequently, mtDNA was extracted according to manufacturer's instructions and
149 dissolved in FG3-buffer.

150 **mtDNA amplification and sequencing**

151 The mtDNA (reference NCBI: NC002333.2) was amplified in three ~5.6kb amplicons
152 (A-C). Fragment A (Forward: CACACCCCTGACTCCCAAAG, Reverse:
153 GGTCGTTTGTACCCGTCAGT) amplified a target spanning nucleotide 16,594 (gene:
154 *trna-pro*) to 5,952 (*nd2*), fragment B (Forward: AAATTAACACCCTAACAACGACCTG,
155 Reverse: GGGGATCAGTACTTTTAGCATTGTAGT) an amplicon from nucleotide
156 5,669 (*nd2*) to 11,319 (*nd4*) and fragment C amplified the mtDNA from nucleotide
157 11,170 (*nd4*) to 295 (*D-loop*). Primers (designed with Primer3) were specific for the
158 mtDNA to avoid the amplification of nuclear-encoded mitochondrial pseudogenes.
159 PCR amplification was performed using Phusion Hot Start II DNA polymerase in GC-
160 buffer (ThermoScientific): 30s at 98°C, followed by 40 cycles of 10s at 98°C
161 (denaturation), 20s at 58°C (annealing) and 8 min at 72°C (extension), with a final
162 step for 10 min at 72°C. The PCR product was checked using electrophoresis on a
163 1% agarose gel containing ethidium bromide, allowing also the detection of large
164 deletions. Amplicons were purified using the Agencourt AMPure XP system
165 (Beckman-Coulter), according to the protocol of the manufacturer. Subsequently, the
166 three purified amplicons were (equimolar) mixed and processed using the
167 customized Nextera XT protocol (McELHOE *et al.* 2014). The library of a random

168 subset of the samples was analyzed using a Bioanalyzer 2100 High Sensitivity DNA
169 chip (Agilent Technologies) to confirm quantity and size of the library. Libraries were
170 indexed and 18 libraries were pooled per lane and analyzed on the HiSeq 2000
171 system (Illumina), using a read length of 1,000 base pairs. PhiX (1%) was spiked in
172 every lane as an internal control.

173 **Pre-processing of Next-Generation sequencing data**

174 As the mtDNA is a multicopy genome (resulting in many biological duplicates),
175 duplicate reads were included in the analysis. Demultiplexing of the data was
176 performed using Illumina CASAVA software (v.1.8.2) and reads were aligned against
177 the mitochondrial reference sequence for the zebrafish (NCBI: NC002333.2) using
178 Burrows-Wheeler Alligner (BWA) software (v.0.5.9) (LI and DURBIN 2010). For variant
179 calling, we used Python 2.6.6., Python Package pysam 0.7.8 and SAMTools 0.1.19.
180 In-house built Perl tools were used to process the variants. As the prevalence of any
181 of the four nucleotides per position was counted to call a variant, the heteroplasmy
182 value was calculated as the ratio of one of the nucleotides over the coverage, which
183 was defined as the total count of any nucleotide at a certain position.

184 **Identification of heteroplasmic *de novo* point mutations**

185 A statistical algorithm was developed to distinguish variant calls from the noise signal,
186 as well as to determine whether point mutations, either a single base substitution or a
187 small insertion or deletion (indel), reported in an oocyte was absent in the
188 corresponding female fish, and thus arose *de novo*. A call from a sample is included
189 in the analysis if its coverage is above the threshold, which is determined by
190 calculating the median coverage for every position of the mtDNA genome, based on
191 the coverage data of all 127 samples (Figure 1). Assuming sequencing quality is
192 independent of the nucleotide position, the median value is the most robust estimate

193 of the coverage across the entire mtDNA genome. This implies that the lowest
194 median coverage value is a robust estimate of the minimal reliable coverage and of
195 the maximum background (noise) signal. As the lowest median coverage value was
196 ~1,700 (Figure 1A), this was chosen as a cut-off value for a position to be included in
197 the analysis, preventing variants with lower coverage from influencing the statistical
198 calculations we applied to exclude false positives.

199 For base substitutions, we discriminated false positives in the higher coverage
200 group from true variants by comparing the percentage heteroplasmy of the variant
201 nucleotide of a particular sample with the average percentage heteroplasmy of all
202 other samples (female tissues and oocytes, but without littermate oocytes and tissues
203 from the mother). To this end, for each substitution a probability distribution of the
204 heteroplasmy values was generated (using all samples) and transformed to a
205 Gaussian distribution using 'a rank-transformation'. We assumed this distribution to
206 be a representation of the noise signal for this variant, which is inherent to the NGS
207 procedure (Guo *et al.* 2013). Hence, we calculated a z-score and *P*-value (one tailed)
208 and considered substitutions with a *P*-value ≤ 0.01 as true variants, being statistically
209 different from the noise signal. The check for *de novo* substitutions was only
210 performed for variants for which the coverage of the oocyte and of ≥ 2 tissues of its
211 mother was $\geq 1,700$. Finally, a substitution was assumed *de novo* if the *P*-value of this
212 variant in the oocyte was ≤ 0.01 , while in the tissues from the corresponding female
213 the *P*-value was > 0.01 (= absent or in noise signal) and if the heteroplasmy
214 percentage was $\geq 1.0\%$.

215 As the sensitivity to identify small indels is at least 2-fold lower as for single
216 nucleotide substitutions (KRAWITZ *et al.* 2010; NEUMAN *et al.* 2013; SENECA *et al.*
217 2015), we only considered *de novo* indels with a coverage $\geq 3,400x$. All suspected *de*

218 *novo* indels were inspected manually, as the software tools used are known be less
219 reliable than for the substitutions, using the Integrative Genomics Viewer (IGV)
220 (THORVALDSDOTTIR *et al.* 2013).

221 **Estimation of mtDNA copy number and mutation rate**

222 From the average heteroplasmy value (het-%) of all *de novo* variants within one
223 mature oocyte, we estimated the mtDNA copy number at the time the mutation
224 occurred. Under the assumption that heteroplasmy levels remain stable during
225 oogenesis, as observed in mice (JENUTH *et al.* 1996) and during stem cell culturing
226 (YAMADA *et al.* 2016) and only one copy is mutated, the mtDNA copy number (z) at
227 the time the mutation occurred can be calculated using: $z = 100/\text{het-\%}$. Subsequently,
228 we aimed to estimate the mutation rate for mutations $\geq 1.5\%$. To do this, we first
229 calculated for every oocyte the total number of detectable nucleotides (y) that were
230 present at the time the mutation arose. Therefore, we multiplied the estimated
231 mtDNA copy number (z) with the number of nucleotides that had coverage $>1,700$: y
232 $= z * [\#\text{nucleotides } >1,700 \text{ coverage}]$. The mutation rate (x) was then calculated by
233 dividing the number of *de novo* mutations in an oocyte by the total number of
234 analyzable nucleotides: $x = [\#\text{mutations detected}] / y$.

235 **Data Availability**

236 The authors state that all detected *de novo* mutations resulting from our statistical
237 analysis are presented within the article.

238 **Results**

239 We studied the occurrence of detectable *de novo* mutations in 103 mature oocytes
240 derived from eight different female zebrafish. No large deletions were observed, but
241 we did detect significant numbers of point mutations. Of the 1,592,714 different

242 nucleotide positions that had a sequence-coverage >1,700, we identified 2,624
243 different base substitutions, which were statistically different from the sequencing
244 noise signal and absent in all three maternal tissues and therefore considered as
245 potential *de novo* mutations. To increase the reliability of our *de novo* base
246 substitution detection, we applied three additional biological filter steps (Figure 1). 1)
247 All oocyte variants for which the heteroplasmy level in one of the corresponding
248 maternal tissues was $\geq 1.0\%$ were considered to be pre-existing and were therefore
249 excluded. 2) The heteroplasmy level of the variants was corrected for the noise signal
250 by subtracting the maternal (M) heteroplasmy level (=the average of the
251 heteroplasmy level in the three maternal tissues) from the oocyte (O) heteroplasmy
252 level (O-M) and variants with small O-M values ($< 1.5\%$) were excluded (205 variants
253 had an O-M value of 1.0-1.5% and 929 variants of $< 1.0\%$). This filter restricted our
254 analysis to *de novo* point mutations with a mutation load $\geq 1.5\%$. 3) A *de novo* variant
255 was rejected if, within the same oocyte, another variant was detected in the two
256 nucleotides adjacent (upstream or downstream) to this variant, as variants located in
257 close proximity to each other are most likely the result of alignment artefacts (LI and
258 DURBIN 2009). By applying these filters, 38 single base substitutions were considered
259 to be *de novo* (Table 2), of which 36 were unique, as two mutations (m.7247T>G and
260 m.10578C>A) were found in two oocytes isolated from the same zebrafish.

261 We also checked for the presence of small *de novo* indels. We did identify
262 three indels with a coverage >3,400: one in oocyte 2.1 (m.7352insC, O-M het: 1.63%,
263 coverage 5,868), one in oocyte 5.10 (m.12323del, O-M het: 1.58%, coverage 3,848)
264 and in oocyte 7.15 (m.11305del, O-M het: 2.41%, coverage 4,689). Using IGV we
265 found that the insertion was only detected in ambiguous reads, while both deletions

266 were only detected in duplicate reads. Therefore, these indels were most likely
 267 alignment artifacts and excluded from further analysis.

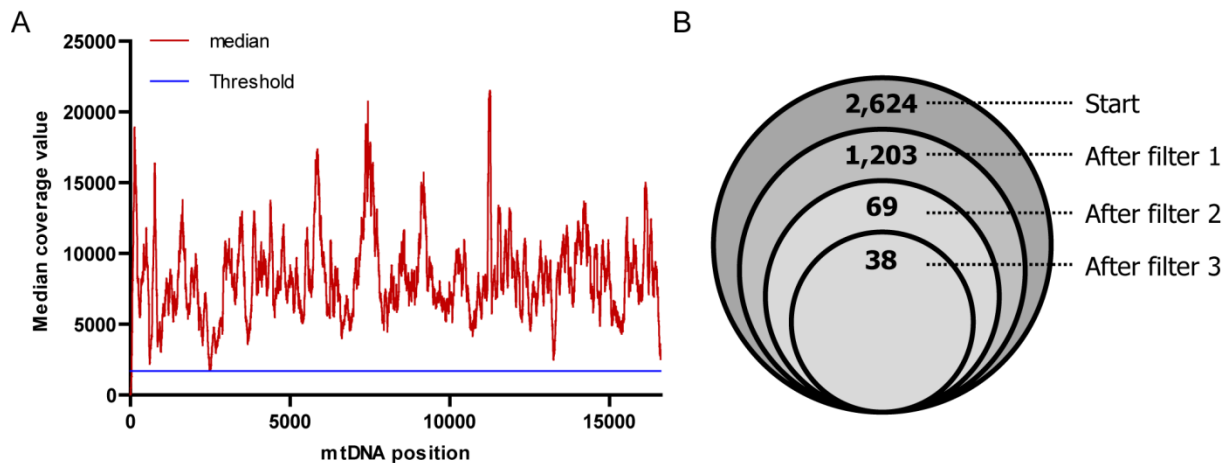
268 The 38 *de novo* mutations were detected in only 19 different oocytes (Table 2),
 269 indicating that the majority (82%) did not have a detectable *de novo* mutation. In
 270 three oocytes (5.2, 5.10 and 7.9) more than three *de novo* mutations were found. No
 271 *de novo* mutations were detected in any oocyte from zebrafish 6. The heteroplasmy
 272 level of all the *de novo* point mutations ranged from 1.5% to 9.0% with an average of
 273 2.7%.

274 **Table 2. Heteroplasmic mtDNA base substitution mutations in all oocytes**

Oocyte ID	Corr. Het-% (O-M)	Gene location	Nucleotide change	Am. Acid change
1.1	2.5%	<i>ND1</i>	m.4164C>A	Ser>STOP
2.3	1.8%	<i>COI</i>	m.6489T>C	Phe>Ser
2.6	5.4%	<i>D-loop</i>	m.250C>T	-
2.6	5.9%	<i>COII</i>	m.8700G>A	Val>Lys
2.10	1.6%	<i>COI</i>	m.6510T>A	Val>Glu
3.2	3.3%	<i>D-loop</i>	m.283G>T	-
3.2	1.9%	<i>ND5</i>	m14296T>A	Ile>Asn
3.9	4.1%	<i>tRNA-Trp</i>	m.6089G>A	-
3.15	1.9%	<i>ND4L/ ND4</i>	m.11303T>A	Stop>Lys Leu>Gln
4.4	3.1%	<i>D-loop</i>	m.1818A>T	-
4.10	1.9%	<i>D-loop</i>	m.532G>A	-
4.10	2.1%	<i>ND4</i>	m.11708G>A	Trp>STOP
5.2	2.7%	<i>ND1</i>	m.4077G>A	Trp>STOP
5.2	2.2%	<i>COI</i>	m.7112C>T	Leu>Phe
5.2	1.6%	<i>COI</i>	m.7247T>G	Trp>Gly
5.2	2.2%	<i>COI</i>	m.7574G>T	Gly>Trp
5.2	2.2%	<i>COI</i>	m.7580G>A	Val>Met
5.3	1.8%	<i>ND6</i>	m.14894T>A	Leu>Phe
5.10	1.6%	<i>12s rRNA</i>	m.1220A>G	-
5.10	2.4%	<i>COI</i>	m.7112C>T	Leu>Phe
5.10	2.1%	<i>COI</i>	m.7247T>G	Trp>Gly
5.10	1.9%	<i>COI</i>	m.7253A>G	Met>Val
5.10	1.8%	<i>COIII</i>	m.9909C>A	Arg>STOP
5.10	1.6%	<i>ND4</i>	m.11500G>C	Val>Leu
5.10	1.5%	<i>tRNA-Leu</i>	m.12838T>G	-
5.10	1.6%	<i>ND5</i>	m.13472C>T	Tyr>Tyr
5.13	8.2%	<i>ND6</i>	m.14761G>A	Leu>Leu

7.3	1.5%	16s rRNA	m.2632A>G	-
7.8	1.7%	16s rRNA	m.2537A>G	-
7.9	2.5%	12s rRNA	m.1550G>C	-
7.9	1.8%	ND4	m.12263T>G	Leu>Arg
7.9	1.6%	ND5	m.13205T>G	Phe>Leu
7.9	1.6%	CytB	m.16232A>C	Thr>Pro
7.9	1.5%	CytB	m.16324A>T	Gly>Gly
8.5	2.8%	ND5	m.14400C>T	Leu>Leu
8.6	9.0%	tRNA-Gly	m.10578C>A	-
8.6	1.5%	ND4	m.12464G>T	Trp>Leu
8.10	4.6%	tRNA-Gly	m.10578C>A	-

275 Corr. Het-%, Oocyte heteroplasmy value corrected from noise signal by subtracting the average
 276 heteroplasmy of the corresponding female tissues from the heteroplasmy value detected in the oocyte.
 277 Am. Acid change, change in amino acid due to change in the codon sequence.



278
 279 **Figure 1. Median reads per position and filtering steps used to determine *de novo* mutations.** A)
 280 Overview of the median reads per position of the mtDNA genome (red line) across all samples. The
 281 blue line indicates the threshold value for the coverage value to include samples. B) Results of filtering
 282 steps performed to determine *de novo* mutations. All reads with coverage above 1,700x (1,592,714
 283 nucleotides) were statistically analyzed, resulting in 2,624 variants with a P -value ≤ 0.01 . Subsequent
 284 filter steps performed: 1) prevalence tissues adult female zebrafish $<1.0\%$, 2) heteroplasmy difference
 285 between tissues from adult zebrafish and her oocytes (O-M) $\geq 1.5\%$ and 3) mutations not detected in
 286 the two nucleotides adjacent (upstream or downstream) of another variant. After filtering, 38 *de novo*
 287 mutations remained.

288 For every mature oocyte with at least one *de novo* mutation, we estimated the
 289 mtDNA copy number present at the time the mutation occurred. This number ranged

290 from 18 to 67 (Table 3). Based on this, we calculated the mutation rate for these
 291 oocytes (Table 3). For most oocytes this mutation rate was in the range of 10^{-6}
 292 mutations per nucleotide, while oocytes 4.4, 5.10 and 7.3 had a higher mutation rate.
 293 On average, the mutation rate in these 19 oocytes was 4.3×10^{-6} mutations per
 294 nucleotide. Strikingly, for oocyte 8.6 the heteroplasmy values of the two reported *de*
 295 *novo* mutations greatly differed from each other, resulting in two different estimations
 296 of the mutation rate.

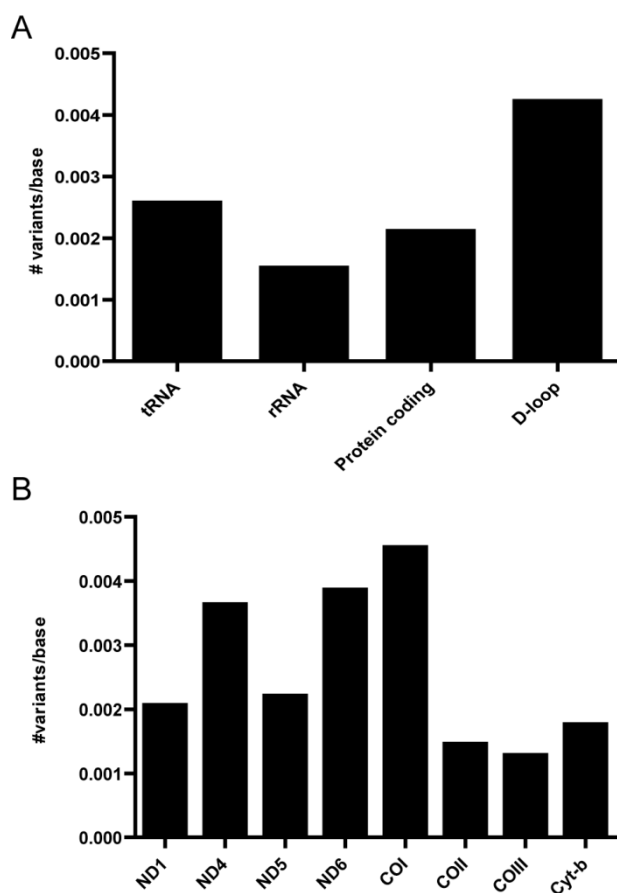
297

298 **Table 3. mtDNA copy number and *de novo* mutation rate $\geq 1.5\%$ at a given**
 299 **nucleotide for all oocytes in which at least one *de novo* mutation was detected**

Oocyte ID	# <i>de novo</i> mutations	Average Het-% of <i>de novo</i> mutation	Copy number from het-%	Positions analyzed (coverage >1700)	Analyzable nucleotides when mutation occurred	Mutation rate (>1.5%) per nucleotide
1.1	1	2.5	40	05,643	225,720	4.4×10^{-6}
2.3	1	1.8	56	16,532	925,792	1.1×10^{-6}
2.6	2	5.7	18	16,580	298,440	6.7×10^{-6}
2.10	1	1.6	63	14,543	916,209	1.1×10^{-6}
3.2	2	1.9	53	16,532	876,196	2.3×10^{-6}
3.9	1	4.1	24	16,555	397,320	2.5×10^{-6}
3.15	1	1.9	53	14,902	789,806	1.3×10^{-6}
4.4	1	3.1	32	02,816	90,112	1.1×10^{-5}
4.10	2	2.0	50	16,583	829,150	2.4×10^{-6}
5.2	5	2.2	45	06,991	314,595	1.6×10^{-6}
5.3	1	1.8	56	12,505	700,280	1.4×10^{-6}
5.10	8	1.7	59	10,740	633,660	1.3×10^{-5}
5.13	1	8.2	12	16,570	198,840	5.0×10^{-6}
7.3	1	1.5	67	16,528	1,107,376	9.0×10^{-7}
7.8	1	1.7	59	16,569	977,571	1.0×10^{-6}
7.9	5	1.8	56	16,426	919,856	5.4×10^{-6}
8.5	1	2.8	36	16,569	596,484	1.7×10^{-6}
8.6*	1	9.0	11	16,239	178,629	5.6×10^{-6}
8.6*	1	1.5	67	16,239	1,088,013	9.2×10^{-7}
8.10	1	4.6	22	16,533	363,726	2.7×10^{-6}
Average	2	3.2	56	-	-	4.3×10^{-6}

300 # *de novo* mutations, number of *de novo* mutations detected in the oocyte. Average Het-% of *de novo*
301 mut., the average heteroplasmy value for all *de novo* mutations found in the oocyte. Copy number
302 from het-%, the copy number the oocytes had when the mutation occurred. *the heteroplasmy values
303 of the variants in oocyte 8.6 differed markedly from each other and therefore the calculations were
304 performed for both heteroplasmy values separately.

305 The number of unique *de novo* mutations per base was assessed for every
306 gene (Figure 2). In case the *de novo* mutations were classified per gene function
307 (tRNA genes, rRNA genes, protein coding or D-loop separately), the prevalence of *de*
308 *novo* mutations appeared to be slightly higher in the D-loop (4 variants per 1000
309 bases). 26 variants were in protein-coding genes (*ND1*, *ND4*, *ND5*, *ND6*, *COI*, *COIII*
310 *and cyt-b*), with little difference in the prevalence among the different protein-coding
311 genes. Four of these mutations were synonymous and 22 non-synonymous,
312 including four mutations leading to a premature stop codon (Table 2).



313

314 **Figure 2. Prevalence of *de novo* variants.** Prevalence A) per gene type (protein coding genes, tRNA,
315 rRNA genes and D-loop) and B) per protein-coding gene. The observed number of variants in all
316 oocytes is expressed as the number of variants per nucleotide. If a *de novo* mutation occurred multiple
317 times, it is only counted once in the construction of these distributions.

318

319 **Discussion**

320 **Robustness of identification *de novo* mutations with heteroplasmy levels $\geq 1.5\%$**

321 We used the Nextera XT protocol to prepare libraries for sequencing on the
322 HiSeq2000 platform, a system which has been successfully applied before for
323 sequencing of the mitochondrial genome (MCELHOE *et al.* 2014; REBOLLEDO-
324 JARAMILLO *et al.* 2014). The identification of specific mutations with low heteroplasmy
325 is limited by the noise level of the sequencing procedure (GUO *et al.* 2013), which is
326 around 1% (GUO *et al.* 2013; REBOLLEDO-JARAMILLO *et al.* 2014; MA *et al.* 2015). As
327 we cannot be sure noise levels will be equal among different runs and detection
328 thresholds differ accordingly, we estimated the noise signal of our sequence run
329 using a non-parametric, data-driven approach. Our approach is twofold. First, we
330 estimated the median minimal coverage (Figure 1), which is a robust estimate of the
331 coverage of the entire mitochondrial genome, rendering a threshold coverage above
332 which the calculated heteroplasmy value is reliable. Second, the noise level of the
333 procedure is estimated for every position in the mtDNA based on the heteroplasmy
334 levels reported for this position in all samples. By applying statistics, this allows
335 identification of those variants for which the heteroplasmy level was significantly
336 different from the background (or noise) signal (P -value ≤ 0.01), thereby excluding
337 variants with a high occurrence in all samples, something which is not expected. In a
338 previous report, power calculations were used to estimate the reliability of the reads

339 (REBOLLEDO-JARAMILLO *et al.* 2014). However, power calculations are theoretical and
340 the use of such post-hoc calculations for the interpretation of available experimental
341 results is debatable (HOENIG and HEISEY 2001). Another step in our analysis involves
342 correction for the noise signal by subtracting the maternal heteroplasmy value from
343 the detected heteroplasmy value. This correction is essential to know at which
344 heteroplasmy value the *de novo* variant arose. A last step involved exclusion of
345 variants that most likely occurred as a result of alignment artefacts. Based on our and
346 others (MCELHOE *et al.* 2014; REBOLLEDO-JARAMILLO *et al.* 2014) experience with next
347 generation sequencing, we excluded variants if they arose in close proximity to each
348 other. Altogether, our data-driven statistical approach allows detection of *de novo*
349 variants (heteroplasmy levels $\geq 1.5\%$) with high reliability, which is corrected for
350 potential differences in quality between sequence runs.

351 ***De novo* mutations are detected in oocytes with a low mtDNA copy number**

352 After applying statistical and biological filters, we characterized 38 *de novo* base
353 substitutions with an average heteroplasmy level of 2.7% in 18% of the oocytes. No
354 large or small indels were detected in our analysis. Our analysis pipeline allowed the
355 detection of variants with a heteroplasmy value $\geq 1.5\%$, which equals detection of a
356 single mutated mtDNA molecule in a population of 65 or less. The estimated mtDNA
357 copy number at which a *de novo* mutation occurred, ranged, based on the detected
358 heteroplasmy levels of the mutations in the oocytes, from 11-67 (Table 2). In our
359 analysis we only detected an mtDNA mutation in 18.9% of the mature oocytes. The
360 inheritance of the mtDNA through a bottleneck leads to low mtDNA levels in
361 primordial germ cells (PGCs) at the bottom of the bottleneck (CREE *et al.* 2008) and a
362 mutation originating at this point may lead to higher heteroplasmy levels. In a
363 previous study (OTTEN *et al.* 2016), we have determined the mtDNA copy number in

364 zebrafish PGCs isolated from several embryonic stages and found, on average, 171
365 mtDNA molecules at the bottom of the bottleneck, but with high variation in this
366 number (StDev: 111). Based on these parameters we constructed a Gaussian
367 distribution with mean 171 and standard deviation 111. As 18.9% of the mature
368 oocytes harbored a *de novo* mutation, this distribution allowed us to estimate that
369 lower 18.9% (left tail of the distribution, z-score -0.88) of the PGCs possess ≤ 72.8
370 mtDNA molecules. An mtDNA copy number of 72.8 correspond to a heteroplasmy
371 level at mutation manifestation of 1.4%, which is close to our detection limit of 1.5%.
372 This means our pipeline allows detection of *de novo* mutations in oocytes that were
373 generated from germ cells with the lowest mtDNA content, which includes those
374 germ cells most prone for acquiring a *de novo* mutation reaching a detectable
375 heteroplasmy of 1.5% or higher, after mtDNA replication. Together, this implies ~20%
376 of the oocytes had a bottleneck size at which *de novo* mutations could reach
377 detectable heteroplasmy levels ($\geq 1.5\%$). This also indicates that the oocytes (the
378 other 82%) with a higher mtDNA copy number will equally carry *de novo* point
379 mutations with a heteroplasmy level $\leq 1.5\%$, but the sensitivity at this level was too
380 low for accurate mtDNA heteroplasmy analysis, which was in line with a recent study
381 (HAMMOND *et al.* 2016). As the current noise level of sequencing is around 1% (GUO
382 *et al.* 2013; REBOLLEDO-JARAMILLO *et al.* 2014; MA *et al.* 2015), further improvements
383 of sequencing technologies are needed to detect mtDNA point mutations in all
384 oocytes, including those with a higher mtDNA copy number.

385 During oogenesis in zebrafish, the mtDNA of the PGC is replicated extensively.
386 mtDNA replication is expected to occur almost exclusively by polymerase gamma
387 (POLG) (COPELAND and LONGLEY 2003; KAGUNI 2004), which is a two-subunit
388 holoenzyme with high fidelity in nucleotide selection and incorporation, alongside with

389 3'-5' exonuclease proofreading functionality (KAGUNI 2004). For all mature oocytes in
390 which we detected a *de novo* mutation, the calculated average mutation rate was
391 4.3×10^{-6} per nucleotide. This is in the same order of the reported POLG error
392 frequencies, which range from 2×10^{-6} to 10×10^{-6} per nucleotide in different animals
393 (KUNKEL and MOSBAUGH 1989; LONGLEY *et al.* 2001). Although POLG has a high
394 accuracy, this suggests that errors made by POLG during the extensive replication
395 during oogenesis are the main cause of *de novo* mutations detected in mature
396 oocytes. The absence of *de novo* indels is in line with a study in human germline
397 mtDNA (REBOLLEDO-JARAMILLO *et al.* 2014) and suggests that error rate of POLG for
398 insertions and deletions is lower than for substitutions, which has been reported
399 before (LONGLEY *et al.* 2001).

400 Although replication errors are made continuously in all oocytes, only
401 replication errors made when mtDNA copy numbers are low (e.g. 65 or lower) lead to
402 detectable (heteroplasmy levels of $\geq 1.5\%$) *de novo* mutations in mature oocytes,
403 which was likely the case in 19 of the oocytes. Four of these oocytes had a higher
404 mutation rate (range of 10^{-5}). Although this can be a chance event, this could also be
405 a reflection of individual differences in error rates of the mtDNA replicative machinery,
406 or due to another mutagenic source being active in these oocytes. During OXPHOS,
407 which is highly active during oogenesis (VAN BLERKOM *et al.* 1995; DUMOLLARD *et al.*
408 2007), mutagenic ROS are being produced and this could be a factor contributing to
409 differences in the mutation rate between oocytes. However, based on the mutation
410 rates in most oocytes, errors made by POLG are most likely the dominant source of
411 *de novo* mtDNA mutations during oogenesis.

412 Our calculations on the mtDNA copy number and mutation rate are only
413 applicable if random processes prevail and every mtDNA molecule is equally

414 amplified. Studies in mice have suggested that heteroplasmy remains stable during
415 oogenesis (JENUTH *et al.* 1996). However, due to genetic drift, leading to loss or
416 fixation of mutations, especially in small sample sizes, and preferential selection,
417 mutation loads can shift. This could explain the high mtDNA mutation load for one of
418 the two *de novo* mutations detected in oocyte 8.6, although these mutations could
419 also have manifested during separate replication cycles, as an extremely low mtDNA
420 bottleneck size creates multiple cycles at which the mutation can manifest at
421 heteroplasmy levels $\geq 1.5\%$. Negative and positive selection has been demonstrated
422 for specific some mutations (STEFFANN *et al.* 2015), further corroborating the
423 possibility that non-random processes also influence the heteroplasmy level of *de*
424 *novo* mtDNA mutations. In the case of selection, the physical and effective bottleneck
425 sizes are different. The mtDNA molecules that actively replicate determine the
426 effective bottleneck size, which can be lower than the physical bottleneck size when
427 selective events result in only a subpopulation of mtDNA molecules being more
428 actively replicated. The mtDNA copy number we have estimated here based on the
429 heteroplasmy levels (11-67) correspond to effective mtDNA copy numbers, and might
430 therefore be an underestimation of the physical bottleneck size.

431 ***De novo* mutations in oocytes are potentially pathogenic**

432 The 38 *de novo* mutations with a frequency of $>1.5\%$ were randomly distributed over
433 the mtDNA genome. After correction for the size of the gene, the *tRNA-Leu*, *tRNA-*
434 *Trp* and *tRNA-Gly* genes had a high number of mutations per nucleotide. However,
435 the numbers were too low to estimate this correctly [only one mutation in the *tRNA-*
436 *Leu* and *tRNA-Trp* genes were observed and two mutations in the *tRNA-Gly* gene]
437 and mutations occurred in two oocytes from the same zebrafish. Furthermore, the
438 tRNA genes as a group do not support a higher prevalence of mutations in the tRNA

439 genes. The observed higher prevalence in the three tRNA genes is most likely due to
440 the relatively small group of *de novo* mutations. On the contrary, a higher prevalence
441 for mutations in the D-loop exists (Figure 2A). This is corroborated by the many
442 variants observed in this mitochondrial control region (CHINNERY *et al.* 1999).
443 Although preferences for the D-loop might exist from an evolutionary perspective,
444 mutations in the mtDNA can arise anywhere in the mtDNA genome. In total, eight
445 protein-coding genes were affected with little differences in the prevalence. 22
446 mutations were non-synonymous, including four mutations leading to a premature
447 stop codon. No differences in prevalence in one of the three codon positions were
448 found. This indicates the effect of a *de novo* mutation can be of any kind. The non-
449 synonymous mutations, especially those causing a premature stop codon, are likely
450 pathogenic, implying that also these severe mutations, which are rarely found in
451 human patients, can occur *de novo*. Most likely in humans, these pathogenic
452 mutations are filtered out by mitophagy (SONG *et al.* 2014) or are at high levels not
453 compatible with embryonic survival and remain at low levels unnoticed.

454 Given the high sequence homology (72%; NCBI blast performed) between the
455 mtDNA genome of zebrafish and humans and the high evolutionary conservation of
456 the mtDNA bottleneck in animal species (WOLFF *et al.* 2011; GUO *et al.* 2013; OTTEN
457 and SMEETS 2015; OTTEN *et al.* 2016) our results indicate that the *de novo* risk might
458 be similar among zebrafish and humans. Indeed, a study in 26 human oocytes
459 (JACOBS *et al.* 2007), 7 oocytes (26.9%) were found to harbor *de novo* variants. This
460 is close to the frequency of 18.9% we report here for zebrafish. This is further
461 corroborated by a similar degree of variation in mtDNA copy number in human
462 oocytes (OTTEN and SMEETS 2015), which suggest also variation in the mtDNA
463 bottleneck size and subsequent differences in the *de novo* risk. In humans, it has

464 been estimated that about 5% of the mutations in the mtDNA alter a conserved
465 nucleotide and are thus potentially pathogenic (JACOBS *et al.* 2007). As we found *de*
466 *novo* mutations in ~20% of the oocytes, this implies ~1% of oocytes will carry a
467 pathogenic *de novo* mutation [with a heteroplasmy level $\geq 1.5\%$]. The presence of
468 low-level mtDNA mutations in the oocyte could, after fertilization, lead to mtDNA
469 disease later in life due to genetic drift, which could lead to fixation of the mutation
470 (GREAVES *et al.* 2014; YIN *et al.* 2015) or in the offspring of the following generation,
471 as inheritance through the mtDNA bottleneck can cause shifts in the heteroplasmy
472 level between mother and child, also leading to fixation of the mutant mtDNA (BLOK
473 *et al.* 1997).

474 Despite the described similarities between zebrafish and humans, important
475 reproductive and mtDNA differences should be taken into account. Zebrafish oocytes
476 (OTTEN *et al.* 2016) possess a much higher absolute mtDNA content as human
477 oocytes (DURAN *et al.* 2011; MURAKOSHI *et al.* 2013) (factor 100), mostly due to
478 different implantation patterns. In humans, implantation occurs rapidly (WIMSATT
479 1975), allowing a fast shift to the uterus for energy supply, while in zebrafish
480 implantation is absent and energy must be supplied by the embryo itself. This lower
481 mtDNA copy number in human oocytes might result in lower mtDNA numbers at the
482 bottom of the bottleneck and the mtDNA genome might be even at higher risk for a
483 *de novo* mutation to reach detectable heteroplasmy levels. This is supported by the
484 high mutation frequency reported for the mammalian mtDNA compared to other
485 animals, including fish (LYNCH 2006). In conclusion, our study in zebrafish has
486 revealed that replication errors made during oogenesis are an important source of *de*
487 *novo* mtDNA mutations and their location and heteroplasmy determine the eventual
488 significance.

489

490 **Acknowledgements**

491 We thank Marie Winandy and H el ene Pendeville from the Zebrafish facility of Li ge
492 University for their assistance in collecting the zebrafish material.

493 **Funding**

494 This work was supported by the Interreg IV program of the European council [the
495 alma-in-silico project to M.M. and H.J.M.S.] and the E-RARE 2 project GENOMIT [R
496 50.02.12F to M.M.]. Part of this work has been made possible with the support of the
497 Dutch Province of Limburg [M.A., M.G. and H.J.M.S.]

498

499 **References**

- 500 Barr, C. M., M. Neiman and D. R. Taylor, 2005 Inheritance and recombination of
501 mitochondrial genomes in plants, fungi and animals. *New Phytol* 168: 39-50.
- 502 Blok, R. B., D. A. Gook, D. R. Thorburn and H. H. Dahl, 1997 Skewed segregation of
503 the mtDNA nt 8993 (T-->G) mutation in human oocytes. *Am J Hum Genet* 60:
504 1495-1501.
- 505 Brand, M. D., 2010 The sites and topology of mitochondrial superoxide production.
506 *Exp Gerontol* 45: 466-472.
- 507 Broughton, R. E., J. E. Milam and B. A. Roe, 2001 The complete sequence of the
508 zebrafish (*Danio rerio*) mitochondrial genome and evolutionary patterns in
509 vertebrate mitochondrial DNA. *Genome Res* 11: 1958-1967.
- 510 Chinnery, P. F., N. Howell, R. M. Andrews and D. M. Turnbull, 1999 Mitochondrial
511 DNA analysis: polymorphisms and pathogenicity. *J Med Genet* 36: 505-510.
- 512 Copeland, W. C., and M. J. Longley, 2003 DNA polymerase gamma in mitochondrial
513 DNA replication and repair. *ScientificWorldJournal* 3: 34-44.
- 514 Cree, L. M., D. C. Samuels, S. C. de Sousa Lopes, H. K. Rajasimha, P. Wonnapijit
515 *et al.*, 2008 A reduction of mitochondrial DNA molecules during
516 embryogenesis explains the rapid segregation of genotypes. *Nat Genet* 40:
517 249-254.
- 518 Dumollard, R., M. Duch en and J. Carroll, 2007 The role of mitochondrial function in
519 the oocyte and embryo. *Curr Top Dev Biol* 77: 21-49.
- 520 Duran, H. E., F. Simsek-Duran, S. C. Oehninger, H. W. Jones, Jr. and F. J. Castora,
521 2011 The association of reproductive senescence with mitochondrial quantity,

522 function, and DNA integrity in human oocytes at different stages of maturation.
523 Fertil Steril 96: 384-388.

524 Greaves, L. C., M. Nooteboom, J. L. Elson, H. A. Tuppen, G. A. Taylor *et al.*, 2014
525 Clonal Expansion of Early to Mid-Life Mitochondrial DNA Point Mutations
526 Drives Mitochondrial Dysfunction during Human Ageing. PLoS Genet 10:
527 e1004620.

528 Guo, Y., C. I. Li, Q. Sheng, J. F. Winther, Q. Cai *et al.*, 2013 Very low-level
529 heteroplasmy mtDNA variations are inherited in humans. J Genet Genomics
530 40: 607-615.

531 Hammond, E. R., M. P. Green, A. N. Shelling, M. C. Berg, J. C. Peek *et al.*, 2016
532 Oocyte mitochondrial deletions and heteroplasmy in a bovine model of ageing
533 and ovarian stimulation. Mol Hum Reprod 22: 261-271.

534 Hellebrekers, D. M., R. Wolfe, A. T. Hendrickx, I. F. de Coo, C. E. de Die *et al.*, 2012
535 PGD and heteroplasmic mitochondrial DNA point mutations: a systematic
536 review estimating the chance of healthy offspring. Hum Reprod Update 18:
537 341-349.

538 Hoenig, J. M., and D. M. Heisey, 2001 The Abuse of Power The Pervasive Fallacy of
539 Power Calculations for Data Analysis Am. Stat. 55: 19-24.

540 Howell, N., S. Halvorson, I. Kubacka, D. A. McCullough, L. A. Bindoff *et al.*, 1992
541 Mitochondrial gene segregation in mammals: is the bottleneck always narrow?
542 Hum Genet 90: 117-120.

543 Jacobs, L., M. Gerards, P. Chinnery, J. Dumoulin, I. de Coo *et al.*, 2007 mtDNA point
544 mutations are present at various levels of heteroplasmy in human oocytes. Mol
545 Hum Reprod 13: 149-154.

546 Jenuth, J. P., A. C. Peterson, K. Fu and E. A. Shoubridge, 1996 Random genetic drift
547 in the female germline explains the rapid segregation of mammalian
548 mitochondrial DNA. Nat Genet 14: 146-151.

549 Kaguni, L. S., 2004 DNA polymerase gamma, the mitochondrial replicase. Annu Rev
550 Biochem 73: 293-320.

551 Kimmel, C. B., W. W. Ballard, S. R. Kimmel, B. Ullmann and T. F. Schilling, 1995
552 Stages of embryonic development of the zebrafish. Dev Dyn 203: 253-310.

553 Krawitz, P., C. Rodelsperger, M. Jager, L. Jostins, S. Bauer *et al.*, 2010 Microindel
554 detection in short-read sequence data. Bioinformatics 26: 722-729.

555 Kunkel, T. A., and D. W. Mosbaugh, 1989 Exonucleolytic proofreading by a
556 mammalian DNA polymerase. Biochemistry 28: 988-995.

557 Lee, H. S., H. Ma, R. C. Juanes, M. Tachibana, M. Sparman *et al.*, 2012 Rapid
558 mitochondrial DNA segregation in primate preimplantation embryos precedes
559 somatic and germline bottleneck. Cell Rep 1: 506-515.

560 Li, H., and R. Durbin, 2009 Fast and accurate short read alignment with Burrows-
561 Wheeler transform. Bioinformatics 25: 1754-1760.

562 Li, H., and R. Durbin, 2010 Fast and accurate long-read alignment with Burrows-
563 Wheeler transform. Bioinformatics 26: 589-595.

564 Longley, M. J., D. Nguyen, T. A. Kunkel and W. C. Copeland, 2001 The fidelity of
565 human DNA polymerase gamma with and without exonucleolytic proofreading
566 and the p53 accessory subunit. J Biol Chem 276: 38555-38562.

567 Lynch, M., 2006 The origins of eukaryotic gene structure. Mol Biol Evol 23: 450-468.

568 Lynch, M., B. Koskella and S. Schaack, 2006 Mutation pressure and the evolution of
569 organelle genomic architecture. Science 311: 1727-1730.

570 Ma, J., H. Purcell, L. Showalter and K. M. Aagaard, 2015 Mitochondrial DNA
571 sequence variation is largely conserved at birth with rare de novo mutations in
572 neonates. *Am J Obstet Gynecol* 212: 530 e531-538.

573 McElhoe, J. A., M. M. Holland, K. D. Makova, M. S. Su, I. M. Paul *et al.*, 2014
574 Development and assessment of an optimized next-generation DNA
575 sequencing approach for the mtgenome using the Illumina MiSeq. *Forensic*
576 *Sci Int Genet* 13: 20-29.

577 Murakoshi, Y., K. Sueoka, K. Takahashi, S. Sato, T. Sakurai *et al.*, 2013 Embryo
578 developmental capability and pregnancy outcome are related to the
579 mitochondrial DNA copy number and ooplasmic volume. *J Assist Reprod*
580 *Genet* 30: 1367-1375.

581 Neuman, J. A., O. Isakov and N. Shomron, 2013 Analysis of insertion-deletion from
582 deep-sequencing data: software evaluation for optimal detection. *Briefings in*
583 *bioinformatics* 14: 46-55.

584 Otten, A. B., and H. J. Smeets, 2015 Evolutionary defined role of the mitochondrial
585 DNA in fertility, disease and ageing. *Hum Reprod Update*.

586 Otten, A. B., T. E. Theunissen, J. G. Derhaag, E. H. Lambrichs, I. B. Boesten *et al.*,
587 2016 Differences in Strength and Timing of the mtDNA Bottleneck between
588 Zebrafish Germline and Non-germline Cells. *Cell Rep* 16: 622-630.

589 Rebolledo-Jaramillo, B., M. S. Su, N. Stoler, J. A. McElhoe, B. Dickins *et al.*, 2014
590 Maternal age effect and severe germ-line bottleneck in the inheritance of
591 human mitochondrial DNA. *Proc Natl Acad Sci U S A* 111: 15474-15479.

592 Sallevelt, S. C., C. E. de Die-Smulders, A. T. Hendrickx, D. M. Hellebrekers, I. F. de
593 Coo *et al.*, 2016 De novo mtDNA point mutations are common and have a low
594 recurrence risk. *J Med Genet*.

595 Seneca, S., K. Vancampenhout, R. Van Coster, J. Smet, W. Lissens *et al.*, 2015
596 Analysis of the whole mitochondrial genome: translation of the Ion Torrent
597 Personal Genome Machine system to the diagnostic bench? *European journal*
598 *of human genetics : EJHG* 23: 41-48.

599 Song, W. H., J. W. Ballard, Y. J. Yi and P. Sutovsky, 2014 Regulation of
600 mitochondrial genome inheritance by autophagy and ubiquitin-proteasome
601 system: implications for health, fitness, and fertility. *Biomed Res Int* 2014:
602 981867.

603 Steffann, J., S. Monnot and J. P. Bonnefont, 2015 mtDNA mutations variously impact
604 mtDNA maintenance throughout the human embryofetal development. *Clinical*
605 *genetics* 88: 416-424.

606 Taylor, R. W., and D. M. Turnbull, 2005 Mitochondrial DNA mutations in human
607 disease. *Nat Rev Genet* 6: 389-402.

608 Thorvaldsdottir, H., J. T. Robinson and J. P. Mesirov, 2013 Integrative Genomics
609 Viewer (IGV): high-performance genomics data visualization and exploration.
610 *Briefings in bioinformatics* 14: 178-192.

611 Van Blerkom, J., P. W. Davis and J. Lee, 1995 ATP content of human oocytes and
612 developmental potential and outcome after in-vitro fertilization and embryo
613 transfer. *Hum Reprod* 10: 415-424.

614 Wimsatt, W. A., 1975 Some comparative aspects of implantation. *Biol Reprod* 12: 1-
615 40.

616 Wolff, J. N., D. J. White, M. Woodhams, H. E. White and N. J. Gemmell, 2011 The
617 strength and timing of the mitochondrial bottleneck in salmon suggests a
618 conserved mechanism in vertebrates. *PLoS One* 6: e20522.

619 Yamada, M., V. Emmanuele, M. J. Sanchez-Quintero, B. Sun, G. Lallo *et al.*, 2016
620 Genetic Drift Can Compromise Mitochondrial Replacement by Nuclear
621 Transfer in Human Oocytes. *Cell stem cell*.

622 Yin, A. H., C. F. Peng, X. Zhao, B. A. Caughey, J. X. Yang *et al.*, 2015 Noninvasive
623 detection of fetal subchromosomal abnormalities by semiconductor
624 sequencing of maternal plasma DNA. *Proc Natl Acad Sci U S A*.

625

626